The Plant Cell, Vol. 24: 4360–4375, November 2012, www.plantcell.org

LARGE-SCALE BIOLOGY ARTICLE

Polypyrimidine Tract Binding Protein Homologs from *Arabidopsis* Are Key Regulators of Alternative Splicing with Implications in Fundamental Developmental Processes[W]

Christina Rühl,[a] Eva Stauffer,[a] André Kahles,[b] Gabriele Wagner,[a] Gabriele Drechsel,[a] Gunnar Rätsch,[b] and Andreas Wachter[a,1]

[a] Center for Plant Molecular Biology, University of Tübingen, 72076 Tuebingen, Germany
[b] Computational Biology Center, Sloan-Kettering Institute, New York, New York 10065

Alternative splicing (AS) generates transcript variants by variable exon/intron definition and massively expands transcriptome diversity. Changes in AS patterns have been found to be linked to manifold biological processes, yet fundamental aspects, such as the regulation of AS and its functional implications, largely remain to be addressed. In this work, widespread AS regulation by *Arabidopsis thaliana* Polypyrimidine tract binding protein homologs (PTBs) was revealed. In total, 452 AS events derived from 307 distinct genes were found to be responsive to the levels of the splicing factors PTB1 and PTB2, which predominantly triggered splicing of regulated introns, inclusion of cassette exons, and usage of upstream 5′ splice sites. By contrast, no major AS regulatory function of the distantly related PTB3 was found. Dependent on their position within the mRNA, PTB-regulated events can both modify the untranslated regions and give rise to alternative protein products. We find that PTB-mediated AS events are connected to diverse biological processes, and the functional implications of selected instances were further elucidated. Specifically, *PTB* misexpression changes AS of *PHYTOCHROME INTERACTING FACTOR6*, coinciding with altered rates of abscisic acid–dependent seed germination. Furthermore, AS patterns as well as the expression of key flowering regulators were massively changed in a PTB1/2 level-dependent manner.

INTRODUCTION

Eukaryotic precursor mRNAs (pre-mRNAs) are subject to extensive co- and posttranscriptional processing, which represents an essential step in the generation of mature, translation-competent mRNAs. Besides its fundamental role in constitutive gene expression, pre-mRNA processing also increases transcriptome complexity by producing distinct mRNA variants from one type of pre-mRNA, thereby providing an additional layer of gene regulation. In particular, alternative pre-mRNA splicing (AS) and alternative 3′ end processing have been found to expand transcriptome diversity enormously in both animals (Mangone et al., 2010; Nilsen and Graveley, 2010) and plants (Reddy, 2007; Hunt, 2011; Syed et al., 2012). While alternative 3′ end processing generates mRNAs of variable lengths, an even more diverse outcome can be achieved by AS via removal of variable single or multiple intronic regions. The resulting splicing variants can vary in their coding regions and in the presence of *cis*-regulatory elements, both of which can have important functional implications.

Among the different types of AS, exon skipping, intron retention, and the use of alternative 5′ and/or 3′ splice sites are most common (Black, 2003; Reddy, 2007). In human, 95% of all intron-containing genes were estimated to be affected by AS (Pan et al., 2008), and recent comprehensive transcriptome analyses based on deep sequencing data revealed a wide extent of AS in plants as well (Filichkin et al., 2010; Lu et al., 2010; Zhang et al., 2010; Marquez et al., 2012). Applying high-throughput RNA sequencing (RNA-seq) techniques, 42 to 61% of all multiexon genes from *Arabidopsis thaliana* (Filichkin et al., 2010; Marquez et al., 2012) and 33 to 48% of all rice (*Oryza sativa*) genes (Lu et al., 2010; Zhang et al., 2010) were found to be associated with AS events. Despite its wide distribution and its huge regulatory potential, many fundamental questions, in particular concerning the control of AS decisions as well as the biological implications of the vast majority of events, remain to be elucidated. AS can, on the one hand, lead to an increase in proteome diversity; however, only few instances in plants have been studied in detail, such as *XBAT35* in *Arabidopsis* (Carvalho et al., 2012). While a comparative analysis of plant splicing variants suggested a minor role of AS in proteome expansion (Severing et al., 2009), the recent identification of many additional splicing variants might lead to a different conclusion. On the other hand, splicing variants can differ in their repertoire of *cis*-regulatory elements with functions in mRNA metabolism and transport. Importantly, many splicing variants display features such as premature termination codons (PTCs) and/or long 3′ untranslated regions (UTRs)

[1] Address correspondence to awachter@zmbp.uni-tuebingen.de.
The author responsible for distribution of materials integral to the findings presented in this article in accordance with the policy described in the Instructions for Authors (www.plantcell.org) is: Andreas Wachter (awachter@zmbp.uni-tuebingen.de).
[W] Online version contains Web-only data.
www.plantcell.org/cgi/doi/10.1105/tpc.112.103622

that are expected to trigger the degradation of these splice forms via the eukaryotic RNA surveillance mechanism nonsense-mediated decay (NMD; Chang et al., 2007; Nicholson et al., 2010). Importantly, NMD not only functions in the clearance of erroneous transcripts originating, for example, from mistakes in transcription or processing, but also enables gene regulation via degradation of AS variants (Lareau et al., 2007). Examples from plants include RNA binding proteins, such as the Gly-rich RNA binding proteins At-GRP7 and -GRP8 (Staiger et al., 2003; Schöning et al., 2008), Ser/Arg-rich (SR) proteins (Kalyna et al., 2003; Palusa and Reddy, 2010), and Polypyrimidine tract binding protein (PTB) homologs (Stauffer et al., 2010). These proteins can act in auto- and cross-regulatory negative feedback loops by triggering splicing of their own pre-mRNA or that of related proteins into an NMD target variant. Interestingly, a previous analysis of transcript features indicated that 43 and 36% of all AS events from *Arabidopsis* and rice, respectively, produce potential NMD targets (Wang and Brendel, 2006). A major role of NMD in targeting AS products was further substantiated by a recent study showing that out of 270 selected genes, 32% generated splicing variants with elevated levels in NMD mutants (Kalyna et al., 2012).

AS decisions are defined by the splicing code, an interaction network of *trans*-acting splicing factors and *cis*-regulatory elements (Chen and Manley, 2009). *Cis*-elements within the pre-mRNA function not only as binding sites for spliceosomal components and regulatory factors, but can also play a more active role in directing splicing, as illustrated by eukaryotic riboswitches (Bocobza et al., 2007; Wachter et al., 2007; Wachter, 2010). Widespread splicing regulatory functions have been assigned to members of the groups of SR and heterogeneous ribonucleoprotein (hnRNP) proteins that often act in a combinatorial manner. While most of our current knowledge on AS regulation is based on animal systems, previous work has provided evidence for the presence of SR (Barta et al., 2008; Reddy and Shad Ali, 2011) and hnRNP proteins (Wachter et al., 2012) and their roles within splicing control in plants. Furthermore, a function of the nuclear cap binding protein complex in controlling AS events in *Arabidopsis* has been demonstrated (Raczynska et al., 2010). Given that several aspects of AS, such as its prevalent types, have been shown to differ between animals and plants (Reddy, 2007), a thorough analysis of the currently ill-defined plant splicing code is of central importance for our understanding of this process (Reddy et al., 2012).

Earlier studies suggested that SR and hnRNP proteins generally act as splicing activators and repressors, respectively. However, more recent work suggested that the splicing regulatory activity can vary for different binding sites as well as for sets of combinatorially acting factors. One example for position-dependent splicing is constituted by the hnRNP protein PTB (Xue et al., 2009; Llorian et al., 2010), an in animals, well-characterized regulator of AS that binds to pyrimidine-rich motifs within pre-mRNAs (Sawicka et al., 2008; Wachter et al., 2012). Evidence has been provided that PTB exploits various mechanisms for AS control, including competing with U2 auxiliary factor 65 in binding to the pre-mRNA (Saulière et al., 2006), looping of RNA regions (Spellman and Smith, 2006), and interference with splicing factor interactions required for exon or intron definition (Izquierdo et al., 2005; Sharma et al., 2005). In animals, a switch in expression from PTB to its neuronal homolog nPTB was shown to reprogram AS patterns and coincides with neuronal development (Boutz et al., 2007). While regulated splicing networks as basis of fundamental biological programs have so far not been characterized in plants, numerous studies supported the occurrence of specific AS patterns linked to certain tissues, development, and stress responses in plants (Palusa et al., 2007; Simpson et al., 2008; Filichkin et al., 2010; Zenoni et al., 2010). Furthermore, important roles of AS control in the regulation of the circadian clock (Sanchez et al., 2010; Staiger and Green, 2011; James et al., 2012) and flowering time (Deng et al., 2010) have been reported.

Interestingly, homologs of PTB proteins are also found in plants. In pumpkin (*Cucurbita maxima*), the PTB homolog RBP50 is translocated from source to sink tissues and was shown to be a component of a phloem-mobile ribonucleoprotein complex (Ham et al., 2009). In *Arabidopsis*, three genes encoding proteins with homology to mammalian PTBs have been identified. Two of these *Arabidopsis* PTB homologs have been suggested to be involved in pollen germination (Wang and Okamoto, 2009), but the underlying molecular basis has not been addressed. While the proteins encoded by *At3g01150* (PTB1) and *At5g53180* (PTB2) are closely related, the protein encoded by *At1g43190* (PTB3) exhibits a quite low level of sequence similarity to the other two. All three PTB homologs from *Arabidopsis* have been shown to generate two types of splice variants of which one encodes the full-length protein, whereas the alternative variant contains a PTC and is subject to degradation via NMD (Stauffer et al., 2010). Based on their ability to alter AS of their own pre-mRNAs in favor of the PTC-containing transcript variant, a model of negative auto- and cross-regulation was proposed (Stauffer et al., 2010; Wachter et al., 2012). Interestingly, comparable regulatory circuits have also been described for the mammalian PTB homologs (Wollerton et al., 2004; Boutz et al., 2007). While these findings provided evidence for the splicing regulatory potential of At-PTBs, a possible existence of further splicing regulation targets as well as the overall functional implications of this group of proteins in *Arabidopsis* remained unresolved.

In this study, we generated a set of transgenic *Arabidopsis* lines having either up- or downregulated PTB levels and subjected these to transcriptome-wide AS analyses. Based on opposite splicing ratio changes in plants with elevated and decreased PTB levels, 452 AS events were identified as potential direct PTB1/2 splicing regulation targets. These AS events comprised mainly alternative 5′ splice site selection, intron retentions, and cassette exons. Independent experimental testing of selected instances confirmed their authenticity. Furthermore, specific as well as redundant splicing regulatory activities of the two closely related proteins PTB1 and PTB2 were established, while no evidence for a major role of PTB3 in splicing control was found. Intriguingly, PTB1/2-regulated AS events are linked to genes with diverse biological functions, and a critical role of some of these AS processes in seed germination and flowering time control was revealed.

RESULTS

Generation of At-*PTB* Misexpression Lines

For the transcriptome-wide identification of potential targets of PTB-mediated splicing regulation, transgenic *Arabidopsis* lines with altered levels of these proteins were generated. *Arabidopsis* mutants with elevated PTB levels were obtained by transformation of Columbia-0 wild-type plants with constructs harboring the coding sequences (cds) of At-*PTB1* (OE1), At-*PTB2* (OE2), or At-*PTB3* (OE3) under control of the constitutive cauliflower mosaic virus promoter. Importantly, use of cds-based constructs prevented the previously described feedback regulation via AS (Stauffer et al., 2010). Downregulation of *PTB* expression was achieved by the transformation of wild-type plants with artificial microRNA (amiRNA) constructs, targeting either the three *PTBs* individually (ami1, ami2, and ami3) or the two closely related homologs *PTB1* and *PTB2* simultaneously (ami1&2; see Supplemental Table 1 online). The amiRNA knockdown approach was chosen as previous work had indicated that single T-DNA mutants in At-*PTB1* and At-*PTB2* have no visible phenotype, while the respective double mutant seemed to be inviable (Wang and Okamoto, 2009).

At least 10 individual T0 generation plants for each construct were analyzed for their *PTB* steady state transcript levels (see Supplemental Figure 1 online). Subsequently, individual lines with minimum and maximum *PTB* transcript levels were selected for further analyses, and alterations in *PTB* expression were confirmed in the following generations (Figure 1A). Relative to the wild-type, *PTB* overexpression resulted in an ~40- and ~15-fold higher level of *PTB1* and *PTB2* transcripts, respectively, while for *PTB3*, only a maximum approximately twofold increase was found. In line with the previously described cross-regulation between PTB1 and PTB2 (Stauffer et al., 2010), strong overexpression of one of these homologs resulted in decreased transcript levels of the other. By contrast, the modest overexpression of *PTB3* did not significantly reduce transcript levels of *PTB1* and *PTB2* and also had no effect on the corresponding protein levels (see below). Upon expression of amiRNAs targeting single *PTBs*, transcript levels of the respective targets were reduced to a minimum of ~30 to 40% in comparison to the wild-type (Figure 1A). The amiRNA construct for simultaneous knockdown of *PTB1* and *PTB2* resulted in a reduction of both mRNAs to ~40% of the wild-type transcript level.

To further characterize the misexpression lines, PTB protein levels were analyzed using affinity-purified polyclonal antibodies. Immunoblot analyses of samples from *Nicotiana benthamiana* leaves transiently expressing Flag-tagged At-PTB1, -PTB2, and

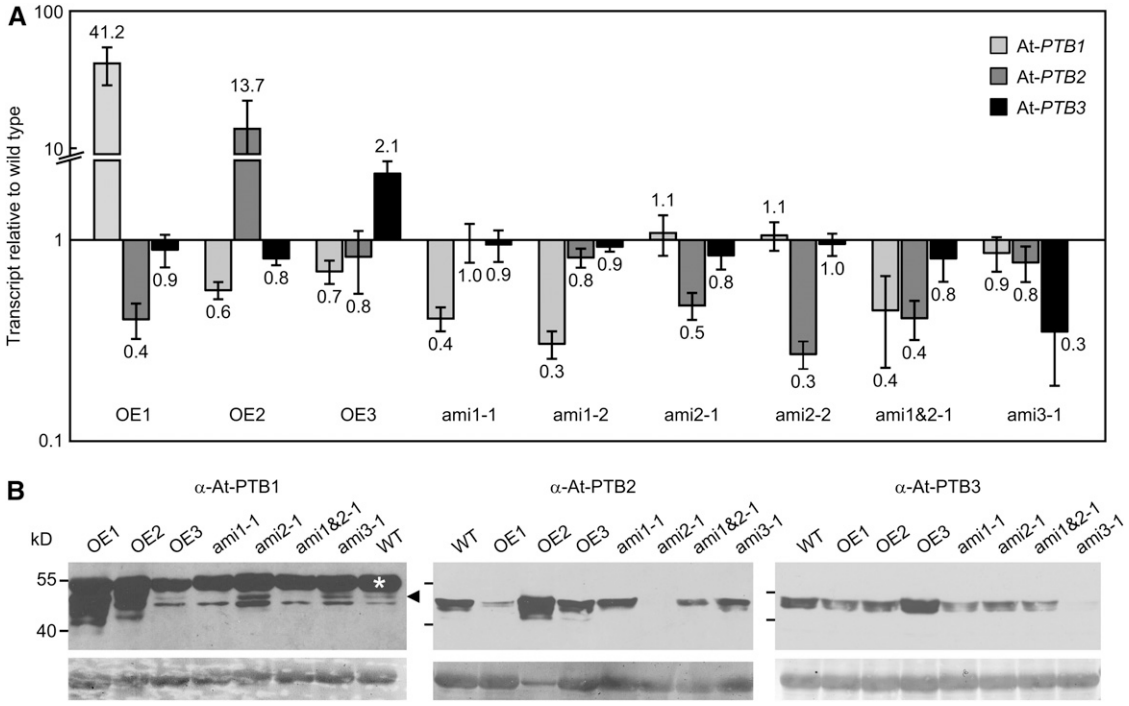

Figure 1. Altered At-PTB Transcript and Protein Levels in Overexpression and amiRNA Lines.

(A) Relative levels of *PTB1*, *PTB2*, and *PTB3* transcripts in either overexpression (OE) or amiRNA (ami) lines for all three At-PTBs, as determined by reverse transcription and quantitative PCR from 10-d-old seedlings. Values are calculated relative to a reference transcript and normalized to wild-type levels. Displayed are mean values (n = 3 to 6) ± SD.

(B) Immunoblot analyses of At-PTB1, -PTB2, and -PTB3 protein levels of samples equivalent to those described in **(A)**. Top panels show immune signals with purified At-PTB–specific antibodies, and bottom panels show amidoblack staining of membranes as loading control. For each sample, 15 μg of total protein was loaded, except for the OE2 sample on the PTB2 blot, for which only 3 μg total protein was loaded. For the PTB1 immunoblot, the white asterisk indicates an unspecific cross-reaction with RBCL protein, and the arrowhead points at the specific PTB1 signal. WT, the wild-type.

-PTB3 yielded strong and specific immune signals in case of the At-PTB2 and At-PTB3 antibodies (see Supplemental Figure 2 online). For the At-PTB1 antibody, an overall weaker signal and cross-detection of the closely related protein At-PTB2 was observed. Analyzing *Arabidopsis* seedlings, PTB1 was barely detectable in the wild-type, but accumulated to high levels in the respective overexpression line (Figure 1B; see Supplemental Figure 3 online). Strong overexpression of PTB2 again resulted in its cross-detection by the At-PTB1 antibody, which was not unexpected regarding the homology of the two proteins. However, a slightly different migration behavior of the two proteins was revealed by extended gel runs, which is in agreement with the calculated molecular weights of 43.6 and 46.9 kD for PTB1 and PTB2, respectively (see Supplemental Figure 3 online). Besides the major immune signal for PTB1 in the OE1 line, several weaker bands corresponding to slightly smaller proteins were detected, which might be due to degradation products and/or posttranslational modifications. Importantly, PTB1 immune signals were not detectable in the ami1 and ami1&2 lines, but, in line with the cross-regulatory potential, showed increased intensity in the ami2 sample. Equivalent results were obtained for PTB2 protein signals, as detected with an At-PTB2–specific antibody (Figure 1B). The same sample set was also analyzed with an At-PTB3–specific antibody, which gave rise to a broad signal at ~50 kD (calculated size: 48.2 kD) in wild-type seedlings (Figure 1B). This signal was strongly reduced in the ami3 line, while a moderate increase in the OE3 seedlings was observed. No major alterations of the PTB3 level in the other lines were found, providing evidence that PTB3 expression does not critically depend on PTB1 and PTB2 levels in seedlings. Estimation of PTB2 and PTB3 protein amounts based on the immune signals for the corresponding overexpression samples revealed an ~9- and 1.5-fold increase, respectively. Specificity of the immune signals was confirmed by analyzing single T-DNA insertion lines for all three *PTBs*, revealing a complete loss of the respective PTB bands (see Supplemental Figures 4 and 5 online). Furthermore, analysis of PTB2 and PTB3 protein levels in the misexpression lines at rosette stage showed that changes persisted during development (see Supplemental Figure 6 online). Interestingly, while PTB3 protein levels in seedlings were not altered upon misexpression of *PTB1* and *PTB2*, we found decreased and increased PTB3 levels in rosette leaves upon *PTB2* overexpression and in the ami1/2 lines, respectively (see Supplemental Figure 6 online). This finding suggests that the cross-regulation between the PTBs varies in a developmental manner. In summary, the immunoblot analyses revealed that PTB protein levels in the misexpression lines were successfully altered, making these lines adequate tools for downstream splicing studies.

Transcriptome-Wide Splicing Studies Reveal a Widespread Regulatory Role of At-PTBs

To identify PTB splicing regulatory targets, RNA-seq analyses of wild-type and *PTB* misexpression lines at seedling stage were performed. The resulting reads (see Supplemental Table 2 online) were mapped to the *Arabidopsis* genome (TAIR10 version), followed by the deduction of information on AS, which led to the identification of 26,076 AS events in total (Figure 2A). We found the usage of alternative 3′ splice sites (alt 3′, 40.6%) to be the most abundant AS type, followed by intron retention (29.8%) and alternative 5′ splice site choice (alt 5′, 21.8%). Finally, only 7.8% of all events were derived from alternative inclusion or skipping of an exon. By contrast, previous RNA-seq–based analyses of AS in *Arabidopsis* identified intron retention to be the most abundant type of AS (Filichkin et al., 2010; Marquez et al., 2012). However, an approximately twofold higher frequency of alt 3′ compared with alt 5′ usage as well as exon skipping being the least abundant among the four basic types of AS analyzed was also reported (Marquez et al., 2012). The varying frequencies of AS types between these studies can be attributed to differences in the biological material, RNA-seq procedures, and read alignments as well as the computational pipelines for defining novel splicing variants.

Analysis of read coverage for the *PTBs* confirmed specific changes in their transcript levels for the corresponding misexpression lines (see Supplemental Figure 7 online). For each AS event, ratios of the two splicing variants were analyzed in pairwise tests, by comparing wild-type, amiRNA, and OE samples and assigning P values to indicate significant changes (see Supplemental Data Set 1 online). We first strictly filtered for events significantly changed in comparison of the amiRNA versus the corresponding OE lines ($P < 0.005$). Subsequent filtering restricted the candidate list to AS events that were also changed in the comparison of wild-type and amiRNA lines, excluding events that only changed upon PTB overexpression and therefore could represent an artifact caused by the excessive supply of a splicing factor. Furthermore, events showing ratio changes in the same direction relative to the wild-type for both amiRNA and OE lines were not further considered. Applying these filter criteria to the ami1&2, OE1, OE2, and wild-type data sets resulted in the identification of 452 AS events being regulated by the closely related PTB1 and PTB2 proteins (Figure 2A). Interestingly, different frequencies of AS types for the PTB1/2-dependent events, in comparison to all AS events, were observed. While cassette exons and alt 5′ events were strongly overrepresented among the PTB1/2-regulated targets, an almost sevenfold decrease in the fraction of alt 3′ events was found. Intriguingly, applying the same filter criteria to the data sets of the corresponding *PTB3* misexpression lines yielded only five AS events derived from four different genes (see Supplemental Data Set 2 online). Independent testing confirmed PTB3-dependent changes in the AS ratio for only two of the five events (see Supplemental Figure 8 online), suggesting that PTB1 and PTB2, but not PTB3 have widespread AS regulatory functions.

Our analysis revealed that certain AS types were overrepresented among the PTB1/2-regulated AS events compared with all detected ones, and we next analyzed the direction of AS change. Downregulation of PTB1 and PTB2 triggered the retention of introns in 77% of all cases from this AS type, while 86% of all regulated cassette exons showed a shift toward the exon skipping version (Figure 2B). For alt 5′ events, PTB1/2 knockdown caused a preferential use of the downstream 5′ splice site, while there was no trend for the few detected PTB1/2-dependent alt 3′ events. Mapping of the AS event positions relative to the TAIR10 representative gene model revealed that

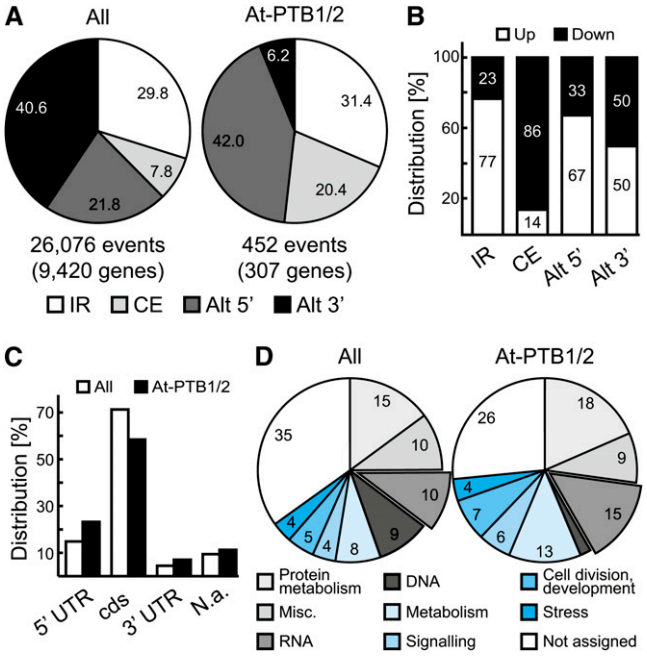

Figure 2. Transcriptome-Wide Identification of At-PTB Splicing Regulation Targets.

(A) Relative frequencies of different AS types for all detected AS events (left) and PTB1/2-regulated events (right). Total numbers of events and associated genes are indicated. alt 5′/3′, alternative 5′/3′ splice site; CE, cassette exon; IR, intron retention.

(B) Direction of splicing change for all At-PTB1/2–regulated AS events in the ami1&2-1 seedlings compared with the wild-type. "Up" and "Down" indicate a relative increase and decrease of the longer splicing variant, respectively.

(C) Frequencies of positions for all and the PTB1/2-regulated AS events in the UTRs and cds of the corresponding TAIR10 representative mRNAs as well as events that could not be implemented (N.a.).

(D) GO term analysis for all genes with a GO assignment and the PTB1/2 regulation targets. Relative proportion of genes with PTB1/2-regulated AS events belonging to GO term "DNA" is 2%.

58, 23, and 7% of the regulated events resided within the cds, 5′ UTR, and 3′ UTR, respectively (Figure 2C; see Supplemental Table 3 online). Compared with all detected events, this represents a higher fraction of UTR positions for the PTB1/2-dependent instances. Furthermore, sequence analyses of the associated splicing variants indicated that 72.3% of the regulated AS events generated at least one transcript form harboring NMD-eliciting features (see Supplemental Table 3 online). Gene ontology (GO) term analysis for the loci associated with PTB1/2-regulated AS events revealed interconnections with diverse biological functions (Figure 2D; see Supplemental Data Set 3 online). Comparing the frequencies of the different GO terms revealed a distinct overrepresentation of the term "RNA" among the PTB1/2 regulation targets relative to all genes, which was most pronounced for the subcategory "RNA processing" (see Supplemental Data Set 3 online). This finding suggests the existence of regulatory networks among genes involved in RNA metabolism with a role of PTB-dependent AS. The GO term "DNA" was clearly underrepresented among the PTB1/2 regulation targets, which can be ascribed to the large number of transposons and transposon-related functions within this GO term group.

To validate our findings of PTB-controlled AS events, representative examples for the different types of AS were selected for independent testing. Out of the 10 analyzed cassette exon events, nine showed reciprocal changes in the proportion of exon inclusion when comparing splicing patterns in the ami1&2-1 and the corresponding OE lines (Figure 3; see Supplemental Figures 9 and 10 online). For *At1g07350*, a pronounced ratio change in the ami1&2, but not in the OE1/2 lines, relative to the wild-type was detected, suggesting that for this event, PTB1 and PTB2 levels might already be saturating in wild-type seedlings. Two of the cassette exon candidates (*At1g07350* and *At1g19800*) were selected based on a previous estimate of exon inclusion rates (data not shown) but did not meet our first stringent filter criterion (the P value was ~0.02 in the comparison of line ami1&2-1 versus OE PTB1/2). Nonetheless, both events could be verified experimentally, suggesting that PTB1/2 regulate even more AS events than estimated based on our stringent filtering. Nine of the tested cassette exons showed an increased ratio of skipping to retention in the ami1&2-1 sample, whereas *At2g34357* showed the opposite direction of change. Furthermore, while downregulation of PTB1/2 had similar quantitative effects for most events, more variation was observed for the OE lines, suggesting that PTB-dependent cassette exons respond differently to varying levels of PTB proteins in vivo. To exclude a general perturbation of AS upon *PTB* misexpression, splice form patterns for the previously characterized cassette exon event within *At1g72050* (Hammond et al., 2009) were determined (Figure 3B).

Our transcriptome-wide splicing studies indicated that the At-PTBs not only regulate cassette exon splicing, as predominantly reported in animals, but also numerous intron retention and alt 5′ events. Therefore, events belonging to these AS-type categories were selected for independent, experimental verification, confirming their authenticity with reciprocal changes in the *PTB1/2* misexpression lines (Figure 4; see Supplemental Figures 10 and 11 online). Alt 3′ events were by far least abundant among the PTB1/2-regulated events; nevertheless, two of these events were selected for independent experimental validation. Splicing variant ratios for wild-type and *PTB1/2* misexpression seedlings were unaltered in case of *At2g13790*, but slightly changed for *At2g43330* (see Supplemental Figures 10 and 12 online).

Subsequently, we determined whether the two close homologs PTB1 and PTB2 act redundantly in splicing regulation and if some of the identified events are also responsive to the distinct homolog PTB3. Therefore, splicing variant ratios of previously described PTB-dependent AS events were determined in seedlings expressing amiRNAs against *PTB1* or *PTB2* (Figure 5A; see Supplemental Figure 13 online). A number of the tested AS events did not show any alteration in the single amiRNA lines compared with the wild-type, suggesting a compensation of the knockdown of either PTB1 or PTB2 by its close homolog. A second category of events showed the same direction of change in the single amiRNA lines as was observed for simultaneous knockdown of PTB1 and PTB2, however, with less pronounced quantitative changes, indicating a redundant function of the two PTBs in the

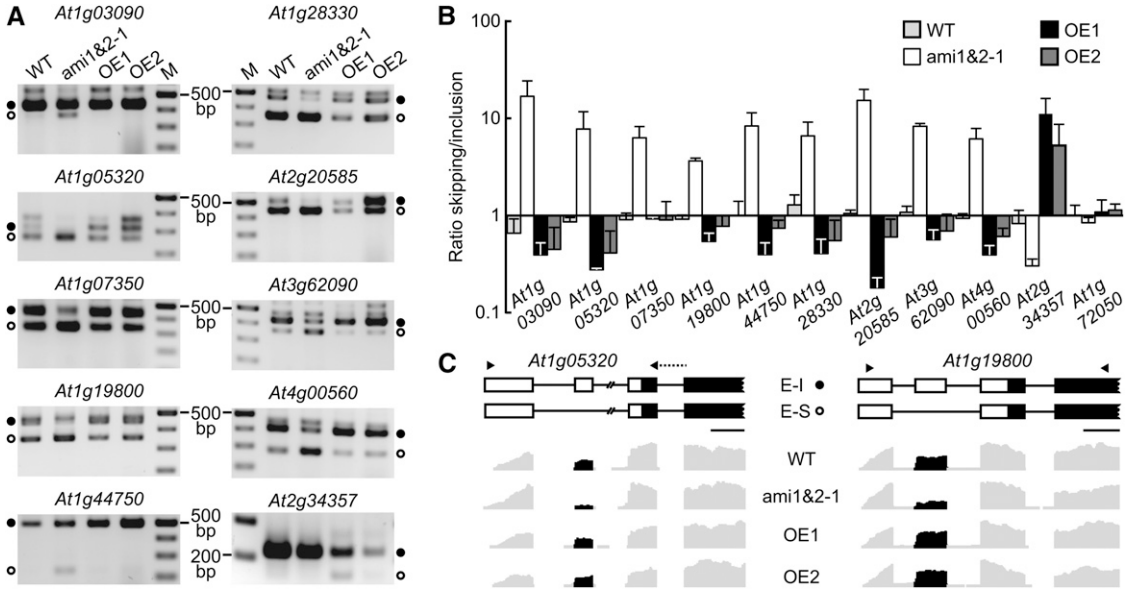

Figure 3. Regulation of Cassette Exon Splicing by At-PTB1 and -PTB2.

(A) RT-PCR analysis of cassette exon splicing ratios for 10 selected genes in seedlings of the genotypes displayed at the top. Black and open circles indicate the bands corresponding to exon inclusion and skipping, respectively. All major bands have been identified by sequencing (see Supplemental Figure 10 online). M designates marker consisting of DNAs in 100 bp increments. WT, the wild-type.

(B) Quantitative analysis of splicing ratios for the candidates shown in **(A)** and a PTB-independent cassette exon event derived from *At1g72050* as negative control using a bioanalyzer. Displayed are mean values (n = 3 to 5) with SD.

(C) Partial gene models depicting the alternatively spliced regions of *At1g05320* and *At1g19800* and corresponding coverage plot areas showing RNA-seq results of the indicated samples. Exon and introns are displayed as boxes and lines, respectively, with black boxes representing cds. Arrows and arrowheads indicate primer binding positions used for coamplification of splicing variants in **(A)** and **(B)**; black lines are scales corresponding to 100 bp length. Coverage plot reads within alternatively spliced region are shown in black, and other reads are in gray.

regulation of these events. For several events in this category, a stronger effect upon PTB2 knockdown was found, suggesting a more dominant regulatory role of this splicing factor compared with PTB1 under the tested conditions. Intriguingly, the cassette exon events associated with the genes *At1g07350* and *At2g20585* showed pronounced opposite ratio changes upon single knockdown of PTB1 or PTB2. These findings strongly suggest that not only the absolute levels of PTB1 and PTB2, but also the ratio of the two proteins have important implications in AS control. Furthermore, analysis of the splicing ratios for selected PTB1/2-regulated AS events showed no or only weak AS changes in the *PTB3* misexpression lines (Figure 5B).

AS of *PIF6* mRNA Is Regulated by At-PTBs and Correlates with Altered Seed Germination

To gain insight into the biological implications of At-PTB–controlled AS events, the list of splicing regulation targets was examined for candidates that have previously been studied with respect to their function, especially regarding the roles of individual splicing variants. One particularly interesting example represented *At3g62090* that encodes PHYTOCHROME INTERACTING FACTOR6 (PIF6) and harbors a PTB1/2-regulated cassette exon event. Studies based on constitutive overexpression of the individual *PIF6* splicing variants had revealed that the exon skipping, but not the inclusion variant, can reduce primary seed dormancy (Penfield et al., 2010). Analysis of *PIF6* AS in different tissues of flowering wild-type plants showed a relative increase of the exon skipping variant in buds compared with leaf tissue (Figure 6A). Downregulation and overexpression of PTB1 and/or PTB2 perturbed *PIF6* mRNA splicing in opposite directions and compromised or fully prevented the tissue-specific AS switch. Furthermore, PTB-linked deregulation of *PIF6* splicing was found in dry seed (Figures 6B and 6C).

To uncover a possible link between *PTB* expression and germination behavior, germination rates of after-ripened seed in the absence or presence of exogenous abscisic acid (ABA) were determined (Figures 6D and 6E; see Supplemental Figure 14 online). While no pronounced difference in seed germination was detectable in the absence of exogenous ABA, elevated and diminished germination rates for the ami1&2-1 and the OE1 lines, respectively, were observed in assays on ABA-containing medium. Interestingly, the changes in germination rates correlated with alterations in AS of the *PIF6* mRNA, which were most pronounced upon simultaneous knockdown of PTB1 and PTB2 as well as overexpression of PTB1. The increased germination rate coincided with a relative increase of the exon skipping variant in the ami1&2-1 plants, being in line with the described germination stimulating effect upon overexpression of this splicing variant. Single knockdown of PTB1 also slightly increased the seed germination rate in the presence of ABA at the early time points (Figure 6E; see Supplemental Figure 14

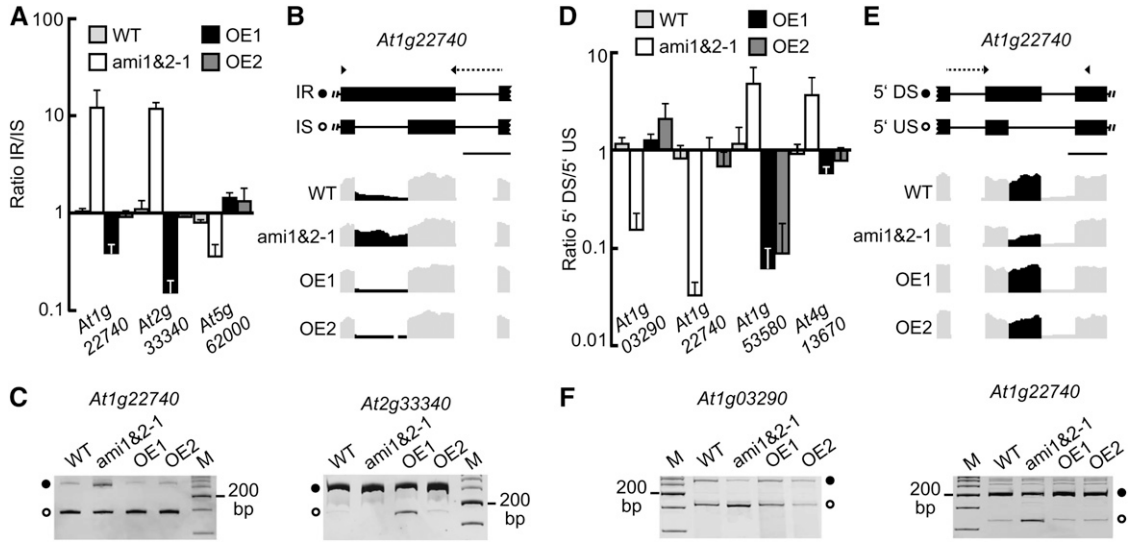

Figure 4. Regulation of Intron Retention and Alternative 5′ Splice Site Choice by At-PTB1 and -PTB2.

(A) Quantitative analysis of transcript ratios for selected intron retention cases in seedlings of genotypes as indicated using a bioanalyzer. Displayed are mean values (n = 3 to 5) with SD. WT, the wild-type; IR, intron retention; IS, intron splicing.

(B) Partial gene model depicting the alternatively spliced region of *At1g22740* and corresponding coverage plot areas showing RNA-seq results of the indicated samples.

(C) RT-PCR analysis of transcript ratios for *At1g22740* and *At2g33340* in seedlings of genotypes as displayed. Black and open circles indicate the bands corresponding to intron retention and splicing, respectively. M, marker consisting of DNAs in 100 bp increments.

(D) Quantitative analysis of transcript ratios for selected alternative 5′ splice site cases as described in **(A)**. DS/US, downstream/upstream splice site.

(E) Partial gene model depicting the region with the two alternative 5′ splice sites for *At1g22740* and corresponding coverage plot areas showing RNA-seq results of the indicated samples.

(F) RT-PCR analysis of transcript ratios for *At1g03290* and *At1g22740* in seedlings of displayed genotypes. Black and open circles indicate the bands corresponding to transcripts derived from the downstream and upstream 5′ splice site, respectively.

online), yet had no effect later on. Consistent with our finding of weak or no ABA-dependent germination effects for the ami1 and ami2 plants, only moderate AS changes for *PIF6* in seedlings (Figure 5A) and dry seed (see Supplemental Figure 14D online) were detected. Overexpression of PTB3 also affected seed germination, yet no opposing effect upon amiRNA knockdown of this homolog was found, speaking against a direct regulatory role. The AS event within *PIF6* leads to inclusion/skipping of an exon within the cds without altering the reading frame and therefore is expected to result in the production of two protein variants. Using a PIF6-specific antibody, we could demonstrate that constitutive expression of the splicing variants in *N. benthamiana* and *Arabidopsis* results in accumulation of proteins of the expected sizes (see Supplemental Figure 14E online), while the PIF6 protein levels in wild-type samples were below the detection limit. Based on these data, the proteins encoded by the *PIF6* splicing variants might accumulate to similar extent in vivo.

To test if At-PTB–mediated AS control of the *PIF6* pre-mRNA is caused by a direct protein/RNA interaction, electrophoretic mobility shift assays (EMSAs) were performed. Using an RNA fragment encompassing the *PIF6* cassette exon and flanking intronic sequences, direct binding of recombinant Thioredoxin-At-PTB2 fusion protein was detected (Figure 7). Control reactions with identical amounts of an unrelated protein of similar size as PTB2 and containing the same Thioredoxin tag did not result in an RNA shift. Interestingly, the analyzed RNA probe contained several polypyrimidine stretches positioned within or downstream of the regulated cassette exon, and further studies need to clarify their putative functions in PTB binding.

At-PTBs Control AS and Expression of Fundamental Flowering Regulator Genes

Splicing of the pre-mRNAs from the flowering regulator genes *FLOWERING LOCUS K* (*FLK*) and *FLOWERING LOCUS M* (*FLM*) was found to be PTB dependent as well. Simultaneous knockdown of *PTB1* and *PTB2* triggered inclusion of an intron within the 5′ UTR of the *FLK* mRNA, while overexpression of *PTB1* had the opposite effect (Figures 8A and 8B). FLK positively regulates flowering by repressing the expression of the flowering repressor *FLOWERING LOCUS C* (*FLC*; Lim et al., 2004; Mockler et al., 2004), and a link between *FLK* pre-mRNA splicing and the expression of *FLC* has been reported previously (Deng et al., 2010). Specifically, an increase of the *FLK* intron retention variant reduced the level of functional FLK protein (Deng et al., 2010), thus resulting in elevated levels of *FLC* expression. Therefore, an increased level of *FLC* expression in the ami1&2-1 plants, displaying a higher rate of FLK intron retention, was anticipated. Intriguingly, the opposite change of *FLC* levels was found, with the *FLC* transcript being undetectable upon PTB1/2 knockdown and strongly elevated in the *PTB1* overexpression plants compared with the wild-type (Figure 8B). Furthermore, an

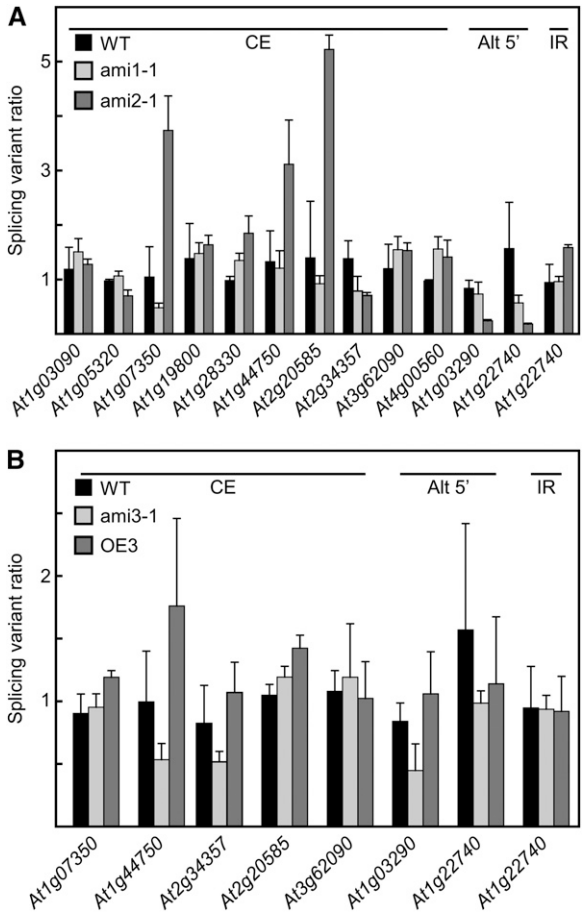

Figure 5. Specific and Redundant Splicing Regulatory Activities of At-PTBs.

(A) Splicing variant ratios in seedling tissues of wild-type (WT), ami1-1-, or ami2-1-expressing plants. Data are mean values (n = 3) with SD of bioanalyzer quantitation. Displayed are examples for cassette exons (CE), alternative 5′ splice site choice (Alt 5′), and intron retention (IR).

(B) Splicing variant ratios of selected PTB1/PTB2-dependent splicing events in *PTB3* misexpression lines. Data are mean values (n = 3) with SD of bioanalyzer quantitation. Other details as described in **(A)**.

altered AS pattern was observed for the pre-mRNA of the *FLC*-like clade member *FLM*, of which one splicing variant has also been reported to encode a floral repressor (Ratcliffe et al., 2001). In the ami1&2-1 plants, an increased level of the mRNA containing the upstream exon was detected (Figure 8B), while levels of the downstream cassette exon splicing variant as well as the coverage within some introns were reduced (Figures 8A and 8B). Thus, the downregulation of *FLC* transcript levels upon knockdown of *PTB1* and *PTB2* is accompanied by AS-mediated down- and upregulation of the floral activator *FLK* and a repressor-encoding *FLM* splicing variant, respectively. Flowering time analysis of *PTB* misexpression lines under short- and long-day conditions revealed that the onset of flowering is unchanged compared with the wild-type (see Supplemental Figure 15 online), suggesting that the changes in positive and negative floral regulators might compensate for each other and/or that additional control mechanisms occur. To assess if the massive increase in *FLC* transcript levels in the OE1 lines might translate into elevated levels of functional FLC protein, read coverage plots were inspected for the occurrence of putative RNA processing variants. Furthermore, four and seven independent, full-length *FLC* cDNA sequences from wild-type and OE1 samples, respectively, were cloned and sequenced. These analyses supported only the occurrence of the representative transcript variant in TAIR10 (*At5g10140.1*). In the absence of any other inhibitory mechanism, this variant should lead to production of functional FLC protein. Moreover, assessment of the levels of the previously reported *COOLAIR* antisense RNAs (Swiezewski et al., 2009) in the *PTB* misexpression lines revealed similar trends of changes as the corresponding sense transcript (see Supplemental Figure 16 online).

DISCUSSION

Regulation of Complex AS Profiles in *Arabidopsis*

Our work identified a few hundred AS events to be specifically altered in their splicing variant ratio output in response to changed levels of the splicing factors PTB1 and PTB2 (Figure 2). Importantly, all of the detected splicing variants were already present in wild-type seedlings, thus not representing artifacts generated by reduced or elevated PTB levels. Recent studies applying high-throughput sequencing techniques revealed that AS is widespread in *Arabidopsis* (Filichkin et al., 2010; Marquez et al., 2012) and AS patterns have been found to be linked to fundamental processes, including abiotic stress responses (Filichkin et al., 2010) and regulation of the circadian clock (Sanchez et al., 2010; James et al., 2012). From these findings, not only a high diversity of AS in plants, but also a prominent role of AS regulation linked to diverse cellular signals can be inferred. While previous studies in plants have mainly addressed the AS regulation for single pre-mRNAs, such as auto- and cross-regulation of At-*GRPs* (Staiger et al., 2003; Schöning et al., 2008), this work provides evidence for complex splicing networks linked to single splicing factors. Considering the huge number of plant splicing regulators, such as the factors belonging to the groups of SR (Barta et al., 2008; Reddy and Shad Ali, 2011) and hnRNP proteins (Wachter et al., 2012), a wide scope of AS in modulating gene expression can be anticipated. Intriguingly, the identified PTB-regulated AS events are associated with genes involved in diverse biological processes, and the functional relevance of selected events has been confirmed in the context of seed germination and flowering control.

Comparing the PTB1/2-dependent to all detected AS events, an overrepresentation of alternative 5′ splice site choice and cassette exons has been found. However, this preference might be linked to these particular splicing factors instead of representing a general bias of regulated AS events. Furthermore, the events found to be regulated by PTB1/PTB2 are located both within the UTRs and the cds and can thus contribute to proteome diversity as well as regulation via UTR-borne signals. Given that a significant fraction of the PTB1/2-regulated transcripts contains NMD-eliciting features, a role of PTBs in gene regulation via coupling of AS and NMD can be anticipated.

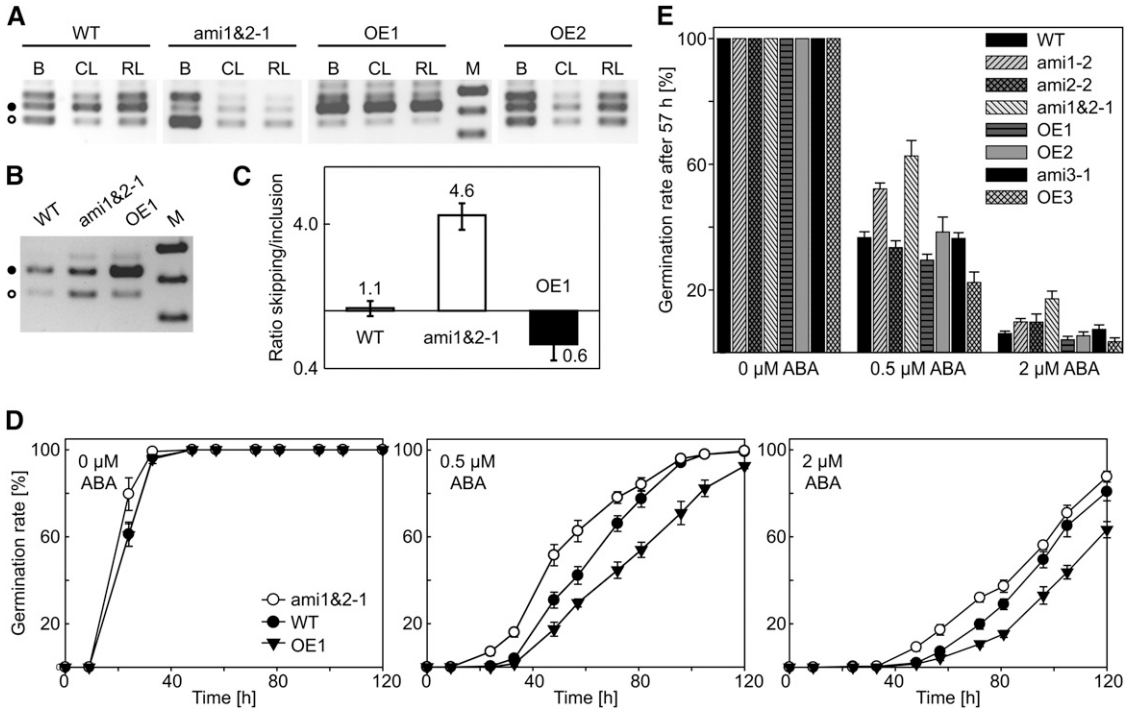

Figure 6. Altered At-PTB Levels Correlate with Changes in *PIF6* Splicing and ABA-Dependent Seed Germination.

(A) RT-PCR analysis of *PIF6* splicing patterns in the wild-type (WT) and the indicated *PTB* misexpression lines for buds (B), cauline leaves (CL), and rosette leaves (RL). M designates marker, and displayed bands correspond to 500, 400, and 300 bp. Black and open circles indicate bands derived from the exon inclusion and skipping variant, respectively.

(B) and **(C)** RT-PCR analysis of *PIF6* splicing in dry seeds from the indicated genotypes. Marker and symbols are as described for **(A)**. RT-PCR products from three independent replicates were quantified using a bioanalyzer **(C)**. Displayed data are mean values ± SD.

(D) Germination assays of wild-type, ami1&2, and OE1 seed in the absence (left panel) or presence of 0.5 µM (middle) or 2 µM (right) ABA in the medium. Data are mean values from three independent experiments and total six replicates; error bars show SE.

(E) Germination rates of the indicated genotypes 57 h after transfer of the seeds to light in the absence or presence of ABA in the medium. Data are mean values from three independent experiments and total six replicates (17 replicates for the wild-type); error bars show SE.

AS Control by At-PTBs

All three At-PTBs have previously been demonstrated to exhibit splicing regulatory potential in an autoregulatory mechanism (Stauffer et al., 2010). Furthermore, the close homologs PTB1 and PTB2 also displayed cross-regulation, while the distantly related PTB3 had no effect on the splicing of the pre-mRNAs of the two other homologs. Our current study further supported the occurrence and specificity of these auto- and cross-regulatory circuits on transcript and protein level (Figure 1) but also suggested development-dependent alterations (see Supplemental Figure 6 online). Interestingly, while a few hundred splicing regulatory targets of PTB1 and PTB2 were identified, only two PTB3-dependent AS events were confirmed. One major difference in comparison of the *PTB1/2* and *PTB3* overexpression lines was only a modest PTB3 increase for the corresponding OE line, compared with the much larger PTB level increase seen in lines OE1 and OE2. However, as our computational analysis for the identification of PTB-dependent AS events was based primarily on splicing ratio changes in lines with diminished PTB levels compared with the wild-type and OE lines, the different overexpression levels are unlikely to explain our finding of a varying extent of AS control by PTBs. Thus, PTB3 might not play a major role in AS control in *Arabidopsis*, but rather have other functions in RNA metabolism. In line with this hypothesis, a pumpkin homolog of At-PTB3 was shown to be part of a phloem-mobile ribonucleoprotein (Ham et al., 2009), the assembly of which requires phosphorylation of the PTB protein (Li et al., 2011).

PTBs have been intensively studied in mammals, where they play an important role during neuronal differentiation (Boutz et al., 2007; Makeyev et al., 2007; Yap et al., 2012). Recent studies indicated that the mode of action of many splicing factors, including PTBs, is highly position dependent (Xue et al., 2009; Llorian et al., 2010). Analyzing inclusion rates of cassette exons, the dominant type of reported AS in mammals, 196 PTB-repressed and 67 PTB-activated instances upon knockdown of PTB in HeLa cells were identified (Llorian et al., 2010). Interestingly, a similar total number of At-PTB1/2–dependent AS events were found in this study, with an overrepresentation of cassette exons compared with all events. In contrast with PTB regulation in mammals, the inclusion of most of these cassette exons was At-PTB1/2–dependent, which is consistent with the

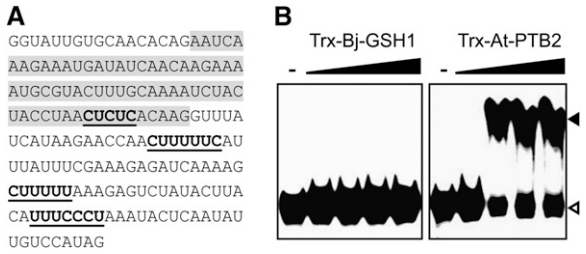

Figure 7. At-PTB2 Binds Directly to an At-*PIF6* RNA Fragment in Vitro.

(A) RNA sequence used for EMSA encompassing the regulated *PIF6* cassette exon (shaded in gray), partial upstream and complete downstream intron, and several pyrimidine-rich stretches (bold and underlined).
(B) EMSA of *PIF6* RNA fragment in the absence of added protein (−), with an unrelated control protein (Trx-Bj-GSH1) or Trx-At-PTB2 fusion protein. Increasing protein concentrations are from left to right. Open and closed arrowheads correspond to free probe and RNA-protein complex, respectively.

previously described auto- and cross-regulation of At-PTB1 and At-PTB2, leading to PTB-dependent inclusion of a poison exon (Stauffer et al., 2010). The opposite mode of autoregulation (i.e., PTB-mediated exon skipping) is found for At-PTB3 (Stauffer et al., 2010) and mammalian PTBs (Wollerton et al., 2004; Spellman et al., 2007). Furthermore, it has been reported that PTB-activated exons typically had PTB binding sites downstream of the exon, while PTB-repressed exons contained pyrimidine motifs upstream of or within the cassette exon (Llorian et al., 2010). Future work needs to address whether there is a similar correlation between binding positions and splicing activities of At-PTBs. Probing of RNA–protein interactions will also reveal if all of the identified targets are directly regulated by At-PTBs, as suggested by the reciprocal AS ratio changes upon up- and downregulation of these splicing factors, or if some alterations are mediated by other, PTB-controlled splicing regulators. In the case of *PIF6*, a direct, in vitro interaction between an RNA probe containing the alternatively spliced region and PTB2 protein was demonstrated (Figure 7).

Besides its well-established role in the regulation of cassette exons, mammalian PTB recently was found to repress splicing of introns within pre-mRNAs of neuron-specific genes (Yap et al., 2012). The resulting mRNAs are recognized as incompletely spliced, leading to their nuclear degradation. We show that At-PTB1 and -PTB2 stimulate and repress intron splicing, as well as alter 5′ splice site choice. However, only few At-PTB1/2–regulated alt 3′ events were identified, suggesting preferential regulation of certain AS types by At-PTBs.

Analysis of plant lines expressing single amiRNAs targeting either At-*PTB1* or -*PTB2* revealed both redundant and specific splicing regulatory functions of the two homologs (Figure 5). In mammals, distinct splicing regulatory activities of PTB and its neuronal homolog nPTB have been reported as an important means for altering gene expression in the course of neuronal differentiation (Boutz et al., 2007; Makeyev et al., 2007). Thus, it will be interesting to see whether relative levels or activities of At-PTB1 and -PTB2 also change in response to certain signals, thereby inducing altered splicing programs.

At-PTB–Mediated *PIF6* Splicing Regulates Seed Germination

The *PIF6* locus generates two splicing variants, encoding predicted proteins either containing or lacking a protein domain due to inclusion or skipping of the corresponding cassette exon. *PIF6* previously has been shown to be expressed during seed development and to have important implications in seed germination (Penfield et al., 2010). Overexpression of the shorter transcript variant, predicted to generate a protein without the DNA binding domain, reduced primary seed dormancy, while no such effect was found for the longer version. Interestingly, we could show that AS of *PIF6* is regulated by PTB1 and PTB2. Misexpression of these splicing regulators perturbed *PIF6* splicing, with increased and reduced levels of exon skipping upon down- and upregulation of PTB1/2, respectively. In line with previous findings (Penfield et al., 2010), a shift toward the shorter variant accelerated seed germination. Furthermore, we observed delayed germination upon change of the splicing ratio into the opposite direction. The seed germination

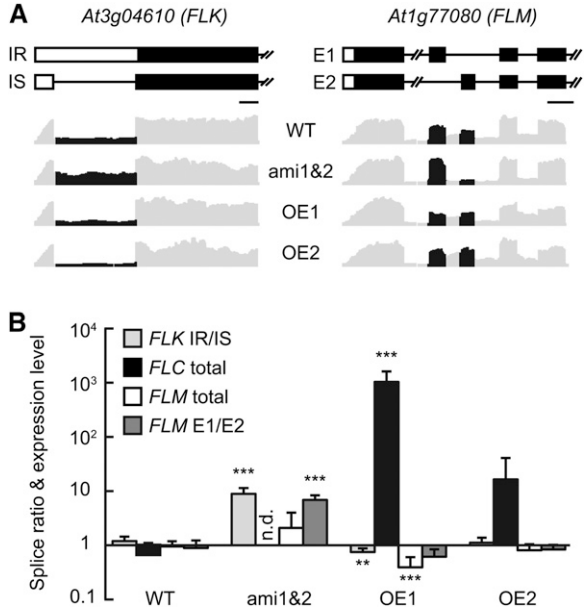

Figure 8. Changes in Splicing Pattern and Expression of the Flowering Regulator Genes *FLK*, *FLC*, and *FLM* in Lines with Altered PTB Levels.

(A) Partial gene models and corresponding coverage plots derived from RNA-seq data for the alternatively spliced regions in the 5′ UTR of the *FLK* (left) and the cds of the *FLM* (right) pre-mRNAs. Details of cartoon depiction as described in legend to Figure 3. WT, the wild-type. IR, intron retention; IS, intron splicing.
(B) Ratio of IR to IS variant of *FLK* mRNA, total levels of *FLC* and *FLM* mRNAs, and ratio of *FLM* splicing isoforms including the first (E1) or second (E2) of the mutually exclusive exons. Values were determined by reverse transcription and quantitative PCR of the indicated genotypes from plants at rosette stage. In the ami1&2 lines, *FLC* mRNA amount was reduced to an undetectable level (n.d.). Data are mean values with SD (n = 5 to 9, each sample derived from three individuals). Highly significant changes compared with corresponding wild-type samples are indicated (***$P < 0.0001$; **$P < 0.0003$ according to Student's t test).

phenotype of the *PTB* misexpression lines depended on the presence of exogenous ABA, and additional links between splicing factors and ABA signaling have recently been reported (Duque, 2011). For example, mutants in the splicing regulator SR45 showed ABA hypersensitivity (Carvalho et al., 2010), and the ABA signaling component *ABSCISIC ACID INSENSITIVE3* was found to be subjected to developmentally controlled AS, with one splicing variant accumulating at the end of seed maturation (Sugliani et al., 2010). Interestingly, *PIF6* showed organ-specific splicing patterns when comparing leaves, flowers, and dry seeds, and these differences were weakened or abrogated in the *PTB* misexpression lines. This organ-specific splicing switch might be due to changes in the expression or activity of PTB1 and PTB2 as well as the involvement of additional splicing factors.

At-*PTB* Misexpression Reveals Intricate Links between AS and Expression for Flowering Regulators

Control of flowering time is crucial for the reproductive success of plants, and numerous previous studies have provided evidence that RNA processing factors play key roles in these complex regulatory networks (Terzi and Simpson, 2008). Accordingly, several links between AS and timing of flowering have been established. The circadian clock component At-GRP7, which autoregulates its own expression via AS, has been described as a novel factor of the autonomous pathway (Streitner et al., 2008) and controls flowering time by repressing the floral repressor FLC (Michaels and Amasino, 1999; Sheldon et al., 1999; Lee et al., 2000). Similarly, FLK also acts as a floral activator by repressing FLC (Lim et al., 2004; Mockler et al., 2004), and recent characterization of the Arg dimethyltransferase *atprmt5* mutant showed that FLK levels, and consequently *FLC* expression, depend on AS of the *FLK* pre-mRNA. While elevated levels of retention of the first intron within *FLK* were found to correlate with *FLC* induction (Deng et al., 2010), the opposite direction of change was found in the *PTB1/2* misexpression lines, suggesting a more complex regulatory relation between *FLK* and *FLC*. The same AS event within *FLK* pre-mRNA was also found to be affected in plants carrying mutations in SERRATE and cap binding complex proteins (Laubinger et al., 2008), further highlighting the multifactorial control of this AS event.

Evidence for additional connections between AS and flowering time control was provided in a study analyzing flowering induction in response to elevated temperature (Balasubramanian et al., 2006). The authors identified *FLM*, a member of the *FLC*-like clade that also represses flowering (Ratcliffe et al., 2001), as a major quantitative trait locus modulating thermal induction of flowering. Furthermore, thermal induction affected the expression of several RNA processing factors, including SR proteins, and led to an altered AS pattern of *FLM*. It was therefore speculated that a shift in AS of *FLM* might provide a mechanism to overcome the repressive effect of FLM in response to elevated temperature, assuming that the splicing variants might have different functional implications. In support of this hypothesis, sequence analysis of the protein isoforms predicted to be produced from the *FLM* splicing variants with mutually exclusive exons revealed the occurrence of distinct interaction motifs (Severing et al., 2012). Interestingly, we also found an alteration of *FLM* splicing upon *PTB1/2* misexpression, with an increase of the splicing variant formerly described as a floral repressor (Ratcliffe et al., 2001) upon simultaneous knockdown of the two close At-PTB homologs. In summary, altered levels of At-PTB1 and -PTB2 resulted in pronounced changes of several key flowering regulators. Knockdown of PTB1/2 caused down- and upregulation of the floral repressors *FLC* and *FLM*, respectively, while AS of the floral inducer *FLK* showed a shift toward an intron retention variant that had previously been demonstrated to be nonfunctional (Deng et al., 2010). We did not find any evidence for alternative processing of *FLC* mRNAs or changes of the corresponding *COOLAIR* antisense transcripts that might counteract the massive alterations in the *FLC* sense transcript levels. Intriguingly, in contrast with the previously described mutants with altered splicing patterns for flowering regulators, the *PTB* misexpression lines flowered at the same time as the wild-type, suggesting compensation of the opposing changes of floral repressors and activators. Our findings thereby further highlight the tight interconnections between these flowering regulators and suggest that AS plays an important role in modulating their expression. Given the observation of simultaneous, compensating changes of AS for several flowering regulators upon alteration of PTB levels, it can be speculated that additional factors are required to specifically change single AS events and thereby affect the onset of flowering. Likely candidate factors are SR proteins, which are known to antagonize hnRNP protein functions in animals. In conclusion, having identified a large and diverse collection of PTB-regulated AS events, future work needs to further elucidate the underlying regulatory mechanism and define complete sets of both *cis*- and *trans*-acting factors. These studies will pave the way for an understanding of the plant splicing code, representing the molecular basis of the highly complex AS patterns linked to manifold biological processes in plants.

METHODS

Plant Growth and Material

For sterile growth, *Arabidopsis thaliana* seeds were surface sterilized with 3.75% NaOCl and 0.01% Triton X-100 and plated on half-strength Murashige and Skoog medium (Duchefa) containing 2% Suc and 0.8% phytoagar (Duchefa). Following stratification for 2 d in darkness at 4°C, plates were transferred to continuous light (~20°C, ~60% humidity). After cultivation for 10 to 12 d, seedlings were sampled or transferred to soil and further grown under long-day growth conditions (16 h light, 8 h darkness, ~20°C, ~60% humidity). *Arabidopsis* was stably transformed using a previously described floral dip method (Clough and Bent, 1998). For selection, seeds were sown on soil followed by spraying of 2- to 3-week-old plants with 0.1% Basta (Bayer) or grown under sterile conditions on medium containing 50 μg/mL kanamycin for plant selection and 200 μg/mL Cefotaxime to prevent bacterial growth. Seeds of following generations were grown under sterile conditions on medium containing 25 μM Basta or 20 μg/mL kanamycin. Single T-DNA insertion lines for At-*PTB1* (*atptb1-1*, SALK_013673C), At-*PTB2* (*atptb2-1*, SAIL_736_B12), and At-*PTB3* (*atptb3-1*, GK-078G10) were obtained from the Nottingham Arabidopsis Stock Centre.

Cloning Procedures

amiRNA constructs to downregulate At-PTB1/2/1&2/3 expression were designed using the WMD3 Web tool (http://wmd3.weigelworld.org;

Ossowski et al., 2008) and cloned using the primers given in the oligonucleotide list (see Supplemental Table 4 online) as described in the provided protocol (http://wmd3.weigelworld.org/downloads/Cloning_of_artificial_microRNAs.pdf). Thereafter, the resulting amiRNA precursors plus flanking vector sequences were recombined into pDONR201 (Invitrogen) via Gateway cloning (Invitrogen). Subsequently, the entry clones were sequenced and recombined into the plant transformation vector pB7WG2 (Karimi et al., 2002).

To clone overexpression constructs of At-*PTB1/2/3*, the respective coding regions were PCR amplified from seedling cDNA using the primers given in Supplemental Table 4 online. The amplification products were digested with *Bam*HI-*Sal*I and cloned into the accordingly digested vector pBinAR (Höfgen and Willmitzer, 1992). For expression of the *PIF6* splicing variants under control of the cauliflower mosaic virus 35S promoter, cds of the four possible splicing variants were cloned into pBinAR via *Bam*HI-*Sal*I. Splicing variants *At3g62090.1* (cassette exon inclusion) and *At3g62090.3* (cassette exon skipping) contain an intron within the 5′ UTR and therefore have a start codon at a later position compared with *At3g62090.2* (cassette exon inclusion). A fourth variant, here named *At3g62090.2/3*, with an early start codon and cassette exon skipping could also be detected. The cds of *At3g62090.1*, *At3g62090.2*, *At3g62090.2/3*, and *At3g62090.3* were amplified with oligos DNA43/44, DNA45/44, DNA45/44, and DNA43/44, respectively, followed by an additional PCR with DNA46 and the listed reverse primers for addition of a complete Flag tag.

To generate antibodies directed against *Arabidopsis* PTB proteins, the coding regions of At-*PTB1*, -*PTB2*, and -*PTB3* were PCR amplified from seedling cDNA using the primers indicated in the oligonucleotide list. The amplification products for *PTB1* and *PTB2* were digested with *Pci*I-*Not*I, whereas the *PTB3* product was digested with *Nco*I-*Not*I. Subsequently, the At-*PTB*–specific inserts were cloned in the *Nco*I-*Not*I–digested expression vector pETM-20 (Hothorn et al., 2003), resulting in constructs encoding Thioredoxin A-His6-tagged PTB proteins with a TEV protease cleavage site. For generation of a PIF6-specific antibody, the cds of the transcript variant *At3g62090.3* was amplified with primers DNA55 and DNA56. The resulting PCR product was digested with *Nco*I-*Kpn*I (using partial digestion as *Nco*I also cuts within the *PIF6* sequence) and cloned into the corresponding sites of pETM-20.

Transient Expression of PIF6 Constructs in *Nicotiana benthamiana*

Transient construct expression was based on a previously described *Agrobacterium tumefaciens*–mediated leaf infiltration assay (Wachter et al., 2007) and included the gene silencing suppressor P19. Samples for protein extraction were taken 5 d after infiltration.

Purification of Recombinant Proteins, Antibody Generation, and Immunoblot Analyses

Recombinant proteins were expressed in the *Escherichia coli* strain *Rosetta gami* DE3 at 16°C overnight, after induction with the following final concentrations of isopropyl-β-D-thiogalactopyranoside: At-PTB1, 0.1 mM; At-PTB2, 0.1 mM; At-PTB3, 0.5 mM; and At-PIF6, 0.1 mM. Bj-GSH1 (Hothorn et al., 2006) was expressed at 28°C overnight after induction with 0.1 mM isopropyl-β-D-thiogalactopyranoside. Protein purification was performed using Ni-TED resin (Macherey-Nagel) according to the manufacturer's instructions. In brief, cell lysis was performed using a French pressure cell (Aminco; 3×, 1000 p.s.i.), and lysates were treated with 50 μg/mL DNase for 15 min at room temperature and subsequently cleared by centrifugation for 30 min at 12,000 rpm and 4°C. For native purification, tagged At-PTB or Bj-GSH1 proteins were bound to Protino Ni-TED resin for 45 min at room temperature. After several washing steps, proteins were eluted first three times with 150 mM imidazole, then three times with 200 mM imidazole. Finally, elution fractions were combined, buffer exchanged to 50 mM NaH_2PO_4 and 200 mM NaCl, pH 8.0, using Zeba desalt spin columns (Pierce), and concentrated (Pierce concentrators, 20 mL/20K) to a final concentration of ~1 mg/mL. Recombinant At-PTB1 and At-PTB2 proteins were directly used for immunization of rabbits, whereas the recombinant At-PTB3 protein was TEV cleaved, followed by removal of the tag by a second column purification step prior immunization. The recombinant PIF6 fusion protein was purified under denaturing conditions. The pellet from the centrifugation after DNase treatment was washed once, followed by resuspension in 50 mM NaH_2PO_4, 300 mM NaCl, and 8 M urea, pH 8.0. After incubation for 1 h at 4°C and centrifugation (20 min at 12,000 rpm and 4°C), the supernatant was incubated with Protino Ni-TED resin for 1 h at room temperature. After several washing steps, proteins were eluted first three times with 200 mM imidazole, then three times with 300 mM imidazole in 8 M urea–containing buffer. Several dialysis steps with decreasing urea concentrations were performed (6, 4, 2, and 0.5 M urea in 50 mM NaH_2PO_4 and 200 mM NaCl, pH 8.0), followed by protein concentration as described above.

Rabbits were immunized at least five times with ~0.1 mg recombinant protein (BioGenes). Antibodies were purified from raw sera by affinity purification using recombinant protein blotted on nitrocellulose membranes. Therefore, raw sera were diluted 1:5 in 2% skim milk in Tris buffered saline (TBS, 20 mM Tris, 150 mM NaCl, pH 7.5), and binding to the antigen was performed at 4°C for 1 h. Subsequently, nitrocellulose stripes were washed three times for 10 min with 2% skim milk-TBS, followed by short washing steps with TBS and water. Antibodies were eluted in two steps by a pH shift. Therefore, stripes were incubated for 3 min in elution buffer 1 (5 mM Gly and 0.5 M NaCl, pH 2.8), and elution was performed on ice with robust shaking. After the first elution, the supernatant was neutralized immediately with Tris, pH 8.0, to a final concentration of 90 mM Tris. The elution was repeated with elution buffer 2 (5 mM Gly and 0.5 M NaCl, pH 2.2), and elution fractions were combined and supplemented with 0.1% BSA. Finally, all elution fractions were concentrated and antibody titers as well as specificities were determined by immunoblotting.

For immunoblot analyses, proteins were extracted from indicated genotypes and tissues using 300 μL extraction buffer (50 mM Tris-HCl, pH 7.5, 150 mM NaCl, 0.1% [v/v] Tween 20, and 0.1% [v/v] β-mercaptoethanol). SDS-PAGE and immunoblots were conducted according to standard protocols using the indicated amounts of total protein, followed by chemiluminescence detection (Super Signal West Dura; Pierce) according to the manufacturer's instructions. For an estimation of protein quantities in the At-PTB overexpression lines, immunoblot signals were quantified using ImageJ (Schneider et al., 2012).

EMSAs

The *PIF6* probe was obtained by in vitro transcription from a PCR-generated DNA template (oligos DNA140/141), followed by 5′ ^{32}P-labeling and gel purification as described before (Wachter et al., 2007). For renaturation, RNA was incubated in 1× binding buffer (20 mM HEPES, 0.2 mM EDTA, 100 mM KCl, 3.125 mM $MgCl_2$, and 20% glycerol [w/v], pH 7.9) for 3 min at 55°C, followed by 5 min at room temperature. Recombinant proteins Trx-At-PTB2 and Trx-Bj-GSH1 (Hothorn et al., 2006) were dialyzed against 1× binding buffer and treated with RNase inhibitor (RiboLock; Fermentas). EMSA reactions of 10 μL total volume contained 10 fmol RNA, 0.1 μg/μL BSA, 3.75 ng/μL tRNA, and varying amounts of purified, recombinant protein (~70 to 200 ng) in 1× binding buffer and were incubated for 10 min at 25°C, followed by native electrophoresis [6% polyacrylamide gel in 0.5× Tris-borate buffer (45 mM Tris, 45 mM borate, 0.5 mM EDTA, pH 8.0) and 5% glycerol] at 4°C for ~3 h and 10 V/cm. Gels were dried and visualized using phosphor imaging (GE Healthcare).

RNA Isolation and RT-PCR Analyses

Total RNA was extracted from ~100 mg of plant tissue using the Universal RNA purification kit (EURx), including an on-column DNaseI treatment

performed according to the manufacturer's instructions. RNA from 75 to 100 mg dry seeds was isolated using a borate extraction protocol as described previously (Penfield et al., 2005). Reverse transcription of total RNA was performed with dT_{20} using AMV reverse transcriptase native (EURx) following the supplied protocol. RT-PCR products were separated and visualized using 2% agarose Tris-acetate (TAE, 40 mM Tris, 20 mM acetate, 1 mM EDTA, pH 8.0) gels or 12% native polyacrylamide gels (Tris-Gly native running buffer) and ethidium bromide staining. For quantification of RT-PCR products, DNA1000 chips on an Agilent 2100 bioanalyzer were used according to the manufacturer's instructions. RT-PCR products were cloned into pGEM-T vector (Promega) before sequencing (Eurofins). Quantitative PCR of cDNA samples was performed using the Bio-Rad CFX384 real-time PCR system and MESA GREEN qPCR Mastermix Plus (Eurogentec) as described previously (Stauffer et al., 2010).

Preparation of TruSeq mRNA Libraries and Illumina Sequencing

Libraries were prepared using the Illumina TruSeq sample prep kit (Illumina) according to the manufacturer's instructions (TruSeq RNA Sample Preparation v2 Guide, version November 2010). Starting materials were 4 to 4.5 µg of total RNA, isolated from 11-day-old seedlings, as described above. For the adapter ligation step, the RNA Adapter Indexes 10 (AR010) and 13 (AR013) were used. Following the PCR enrichment step using half the sample volume, libraries were subjected to an additional gel purification step. A size range of 250 to 350 bp was extracted from a 2% agarose gel and purified using the MinElute gel extraction kit (Qiagen). Cluster generation was performed on a Cluster Station (Illumina) or cBot (Illumina) according to the manufacturer's instructions. Sequencing was performed with one sample per lane, and 8 to 10 pM solutions of denatured libraries were used to generate ~800,000 raw clusters per mm^2 on the flow-cell surface. Sequencing was performed according to the manufacturer's protocols on a Genome Analyzer GAIIx (Illumina) using the TruSeq SBS Sequencing Kit v5 (36 cycle; Illumina). Sequencing control software was SCS version 2.8 and RTA1.8.7. Sequencing runs were performed at 80-bp cycles or 100-bp cycles. For further details, see Supplemental Methods 1 online.

RNA-seq Data Analysis

The RNA-seq read data were aligned to the *Arabidopsis* reference genome (TAIR10) using the spliced alignment tool PALMapper (Jean et al., 2010). Further postprocessing to achieve an optimal filter setting and to resolve multimappers to unique locations was done using the RNA-geeq toolbox (http://bioweb.me/rnageeq). The TAIR10 annotation was transformed into a splicing graph representation and was augmented with additional splice evidence from alignment data using Spladder. Canonical AS events were extracted from the generated splicing graph and transformed into genelets (a minimal gene with two transcript isoforms). Differential testing of alternative splice isoform expression and differential gene expression estimation based on negative binomial tests taking biological variance into account were made with rDiff (Stegle et al., 2010; http://bioweb.me/rDiff) and DESeq (Anders and Huber, 2010), respectively, on the aforementioned genelets. The resulting ranked lists for different conditions were combined in a spreadsheet program. For NMD feature evaluation, an analysis pipeline was implemented in MATLAB, Python, and as shell scripts. For further details, see Supplemental Methods 1 online.

Functional Clustering of At-PTB1/2–Regulated Genes

Functional clustering was performed using the MapMan software (http://mapman.gabipd.org; Thimm et al., 2004). All analyzed genes were assigned a gene function based on the corresponding GO terms listed in TAIR10. Based on these GO terms, genes were clustered in 35 different functional groups and further combined as depicted in Supplemental Data Set 3 online.

Germination Assays

Seeds from 10 plants of each genotype simultaneously grown under greenhouse conditions were harvested at the same time and after-ripened at 4°C for at least 2 months. For each experiment, 80 to 100 seeds of each genotype were surface sterilized for 5 min and sown on half-strength Murashige and Skoog medium (as described above) containing ABA (Sigma-Aldrich) in the indicated concentrations. ABA was dissolved in 100% methanol, and a volume of methanol corresponding to the highest ABA concentration was added to the control medium. After stratification for 2 d in darkness at 4°C, plates were transferred to a long-day growth chamber (~20°C, ~60% humidity, 16 h light). Seeds were scored as germinated at the stage of radicle emergence.

Flowering Time Determination

Seeds of each genotype were sown on soil and transferred to short-day (8 h light) or long-day (16 h light) conditions after stratification for 2 d in darkness at 4°C. For each genotype and growth condition, nine to 20 plants were transferred to single pots 2 weeks after transfer to light and arranged randomly to avoid positional variations of growth conditions. Plants were scored as flowering once inflorescence stems reached a length of 1 cm. Flowering time was determined by counting rosette leaf numbers or days after transfer to light, for long- and short-day conditions, respectively.

Accession Numbers

Sequence data for genes in this article can be found in The Arabidopsis Information Resource databases under the following accession numbers: *PTB1* (*At3g01150*), *PTB2* (*At5g53180*), *PTB3* (*At1g43190*), *PIF6* (*At3g62090*), *FLK* (*At3g04610*), *FLC* (*At5g10140*), and *FLM* (*At1g77080*). Accession numbers of further analyzed genes are given in Figures 3 and 4 and Supplemental Figures 8, 9, 11, and 12 online. Supplemental Data Sets 1 to 3 online are available at datadryad.org (doi:10.5061/dryad.6k1p6). RNA-seq data have been deposited in the Gene Expression Omnibus repository (http://www.ncbi.nlm.nih.gov/geo) under accession number GSE41433.

Supplemental Data

The following materials are available in the online version of this article.

Supplemental Figure 1. Altered At-*PTB* Transcript Levels in amiRNA and Overexpression Lines of T0 Generation.

Supplemental Figure 2. Specificities of Purified At-PTB Antibodies.

Supplemental Figure 3. Exposure Time-Dependent At-PTB1 Immunosignals.

Supplemental Figure 4. Genotyping and Immunoblot Analyses of At-*PTB* T-DNA Insertion Lines.

Supplemental Figure 5. Mapping of T-DNA Positions in At-*PTB1*, -*PTB2*, and -*PTB3* Insertion Lines.

Supplemental Figure 6. PTB2 and PTB3 Protein Levels in *PTB* Misexpression Lines at the Rosette Stage.

Supplemental Figure 7. RNA-seq–Based *PTB* Expression Analysis in the Corresponding Misexpression Lines.

Supplemental Figure 8. Validation of Putative PTB3 Splicing Regulation Targets.

Supplemental Figure 9. Partial Gene Models and Corresponding Coverage Plots for Described Cassette Exon Events.

Supplemental Figure 10. Sequences of Main RT-PCR Products Corresponding to Described Splicing Variants.

Supplemental Figure 11. Partial Gene Models and Corresponding Coverage Plots for Selected Intron Retention and Alternative 5′ Splice Site Events.

Supplemental Figure 12. Validation of PTB1/2 Functioning in Alternative 3′ Splice Site Choice.

Supplemental Figure 13. Visualization of RT-PCR Products for Alternative Splicing Events in Single amiRNA and *PTB3* Misexpression Lines.

Supplemental Figure 14. Germination Assays of Wild-Type and *PTB* Misexpression Lines and AS Products of *PIF6*.

Supplemental Figure 15. Flowering Time Analysis of *PTB* Misexpression Lines under Long- and Short-Day Conditions.

Supplemental Figure 16. Analysis of *FLC* Antisense Expression in Wild-Type and *PTB* Misexpression Lines.

Supplemental Table 1. Overview of Utilized amiRNAs and Their Targets.

Supplemental Table 2. Read Statistics of RNA-seq Data.

Supplemental Table 3. Frequencies of AS Event Positions in the mRNA and NMD Features.

Supplemental Table 4. List of Oligonucleotides.

Supplemental Methods 1. Sequencing of mRNA Libraries and Computational Methods.

Supplemental Data Set 1. Computational Analysis of Transcriptome-Wide AS Patterns in *PTB1/2* Misexpression Lines.

Supplemental Data Set 2. Computational Analysis of Transcriptome-Wide AS Patterns in *PTB3* Misexpression Lines.

Supplemental Data Set 3. Detailed List of GO Terms.

ACKNOWLEDGMENTS

We thank Christa Lanz, Jens Riexinger, and the Genome Center (Max Planck Institute, Tuebingen, Germany) for performing the Illumina sequencing, Philipp Drewe for sharing an unpublished method and contributing code, Vipin T. Sreedharan for visualization of RNA-seq data, and Markus Schmid for providing seeds of the *flc-3* mutant. Furthermore, we thank Natalie Faiss, Charlotte Ost, and the central facilities of the Center for Plant Molecular Biology (Center for Plant Molecular Biology, University of Tuebingen) for technical support. This work was funded by Emmy Noether Fellowship WA 2167/2-1 and Deutsche Forschungsgemeinschaft Grant RA1894/2-1.

AUTHOR CONTRIBUTIONS

C.R., E.S., G.R., and A.W. designed research. C.R., E.S., A.K., G.W., G.D., G.R., and A.W. performed research. All authors contributed to data analysis and discussion. A.W., C.R., and E.S. wrote the article.

Received August 1, 2012; revised October 9, 2012; accepted October 24, 2012; published November 27, 2012.

REFERENCES

Anders, S., and Huber, W. (2010). Differential expression analysis for sequence count data. Genome Biol. **11:** R106.

Balasubramanian, S., Sureshkumar, S., Lempe, J., and Weigel, D. (2006). Potent induction of *Arabidopsis thaliana* flowering by elevated growth temperature. PLoS Genet. **2:** e106.

Barta, A., Kalyna, M., and Lorković, Z.J. (2008). Plant SR proteins and their functions. Curr. Top. Microbiol. Immunol. **326:** 83–102.

Black, D.L. (2003). Mechanisms of alternative pre-messenger RNA splicing. Annu. Rev. Biochem. **72:** 291–336.

Bocobza, S., Adato, A., Mandel, T., Shapira, M., Nudler, E., and Aharoni, A. (2007). Riboswitch-dependent gene regulation and its evolution in the plant kingdom. Genes Dev. **21:** 2874–2879.

Boutz, P.L., Stoilov, P., Li, Q., Lin, C.H., Chawla, G., Ostrow, K., Shiue, L., and Ares, M. Jr., and Black, D.L. (2007). A post-transcriptional regulatory switch in polypyrimidine tract-binding proteins reprograms alternative splicing in developing neurons. Genes Dev. **21:** 1636–1652.

Carvalho, R.F., Carvalho, S.D., and Duque, P. (2010). The plant-specific SR45 protein negatively regulates glucose and ABA signaling during early seedling development in *Arabidopsis*. Plant Physiol. **154:** 772–783.

Carvalho, S.D., Saraiva, R., Maia, T.M., Abreu, I.A., and Duque, P. (May 24, 2012). XBAT35, a novel *Arabidopsis* RING E3 ligase exhibiting dual targeting of its splice isoforms, is involved in ethylene-mediated regulation of apical hook curvature. Mol. Plant http://dx.doi.org/10.1093/mp/sss048.

Chang, Y.F., Imam, J.S., and Wilkinson, M.F. (2007). The nonsense-mediated decay RNA surveillance pathway. Annu. Rev. Biochem. **76:** 51–74.

Chen, M., and Manley, J.L. (2009). Mechanisms of alternative splicing regulation: insights from molecular and genomics approaches. Nat. Rev. Mol. Cell Biol. **10:** 741–754.

Clough, S.J., and Bent, A.F. (1998). Floral dip: A simplified method for Agrobacterium-mediated transformation of *Arabidopsis thaliana*. Plant J. **16:** 735–743.

Deng, X., Gu, L., Liu, C., Lu, T., Lu, F., Lu, Z., Cui, P., Pei, Y., Wang, B., Hu, S., and Cao, X. (2010). Arginine methylation mediated by the *Arabidopsis* homolog of PRMT5 is essential for proper pre-mRNA splicing. Proc. Natl. Acad. Sci. USA **107:** 19114–19119.

Duque, P. (2011). A role for SR proteins in plant stress responses. Plant Signal. Behav. **6:** 49–54.

Filichkin, S.A., Priest, H.D., Givan, S.A., Shen, R., Bryant, D.W., Fox, S.E., Wong, W.K., and Mockler, T.C. (2010). Genome-wide mapping of alternative splicing in *Arabidopsis thaliana*. Genome Res. **20:** 45–58.

Ham, B.K., Brandom, J.L., Xoconostle-Cázares, B., Ringgold, V., Lough, T.J., and Lucas, W.J. (2009). A polypyrimidine tract binding protein, pumpkin RBP50, forms the basis of a phloem-mobile ribonucleoprotein complex. Plant Cell **21:** 197–215.

Hammond, M.C., Wachter, A., and Breaker, R.R. (2009). A plant 5S ribosomal RNA mimic regulates alternative splicing of transcription factor IIIA pre-mRNAs. Nat. Struct. Mol. Biol. **16:** 541–549.

Höfgen, R., and Willmitzer, L. (1992). Transgenic potato plants depleted for the major tuber protein patatin via expression of antisense RNA. Plant Sci. **87:** 45–54.

Hothorn, M., Bonneau, F., Stier, G., Greiner, S., and Scheffzek, K. (2003). Bacterial expression, purification and preliminary X-ray crystallographic characterization of the invertase inhibitor Nt-CIF from tobacco. Acta Crystallogr. D Biol. Crystallogr. **59:** 2279–2282.

Hothorn, M., Wachter, A., Gromes, R., Stuwe, T., Rausch, T., and Scheffzek, K. (2006). Structural basis for the redox control of plant glutamate cysteine ligase. J. Biol. Chem. **281:** 27557–27565.

Hunt, A.G. (2011). RNA regulatory elements and polyadenylation in plants. Front. Plant Sci. **2:** 109.

Izquierdo, J.M., Majós, N., Bonnal, S., Martínez, C., Castelo, R., Guigó, R., Bilbao, D., and Valcárcel, J. (2005). Regulation of Fas alternative splicing by antagonistic effects of TIA-1 and PTB on exon definition. Mol. Cell **19:** 475–484.

James, A.B., Syed, N.H., Bordage, S., Marshall, J., Nimmo, G.A., Jenkins, G.I., Herzyk, P., Brown, J.W., and Nimmo, H.G. (2012). Alternative splicing mediates responses of the *Arabidopsis* circadian clock to temperature changes. Plant Cell **24:** 961–981.

Jean, G., Kahles, A., Sreedharan, V.T., De Bona, F., and Ratsch, G. (2010). RNA-Seq read alignments with PALMapper. Curr. Protoc. Bioinformatics **32:** 11.6.1–11.6.37.

Kalyna, M., Lopato, S., and Barta, A. (2003). Ectopic expression of atRSZ33 reveals its function in splicing and causes pleiotropic changes in development. Mol. Biol. Cell **14:** 3565–3577.

Kalyna, M., et al. (2012). Alternative splicing and nonsense-mediated decay modulate expression of important regulatory genes in *Arabidopsis*. Nucleic Acids Res. **40:** 2454–2469.

Karimi, M., Inzé, D., and Depicker, A. (2002). GATEWAY vectors for Agrobacterium-mediated plant transformation. Trends Plant Sci. **7:** 193–195.

Lareau, L.F., Brooks, A.N., Soergel, D.A., Meng, Q., and Brenner, S.E. (2007). The coupling of alternative splicing and nonsense-mediated mRNA decay. Adv. Exp. Med. Biol. **623:** 190–211.

Laubinger, S., Sachsenberg, T., Zeller, G., Busch, W., Lohmann, J.U., Rätsch, G., and Weigel, D. (2008). Dual roles of the nuclear cap-binding complex and SERRATE in pre-mRNA splicing and microRNA processing in *Arabidopsis thaliana*. Proc. Natl. Acad. Sci. USA **105:** 8795–8800.

Lee, H., Suh, S.S., Park, E., Cho, E., Ahn, J.H., Kim, S.G., Lee, J.S., Kwon, Y.M., and Lee, I. (2000). The AGAMOUS-LIKE 20 MADS domain protein integrates floral inductive pathways in *Arabidopsis*. Genes Dev. **14:** 2366–2376.

Li, P., Ham, B.K., and Lucas, W.J. (2011). CmRBP50 protein phosphorylation is essential for assembly of a stable phloem-mobile high-affinity ribonucleoprotein complex. J. Biol. Chem. **286:** 23142–23149.

Lim, M.H., Kim, J., Kim, Y.S., Chung, K.S., Seo, Y.H., Lee, I., Kim, J., Hong, C.B., Kim, H.J., and Park, C.M. (2004). A new *Arabidopsis* gene, FLK, encodes an RNA binding protein with K homology motifs and regulates flowering time via FLOWERING LOCUS C. Plant Cell **16:** 731–740.

Llorian, M., Schwartz, S., Clark, T.A., Hollander, D., Tan, L.Y., Spellman, R., Gordon, A., Schweitzer, A.C., de la Grange, P., Ast, G., and Smith, C.W. (2010). Position-dependent alternative splicing activity revealed by global profiling of alternative splicing events regulated by PTB. Nat. Struct. Mol. Biol. **17:** 1114–1123.

Lu, T., Lu, G., Fan, D., Zhu, C., Li, W., Zhao, Q., Feng, Q., Zhao, Y., Guo, Y., Li, W., Huang, X., and Han, B. (2010). Function annotation of the rice transcriptome at single-nucleotide resolution by RNA-seq. Genome Res. **20:** 1238–1249.

Makeyev, E.V., Zhang, J., Carrasco, M.A., and Maniatis, T. (2007). The microRNA miR-124 promotes neuronal differentiation by triggering brain-specific alternative pre-mRNA splicing. Mol. Cell **27:** 435–448.

Mangone, M., et al. (2010). The landscape of C. elegans 3'UTRs. Science **329:** 432–435.

Marquez, Y., Brown, J.W., Simpson, C., Barta, A., and Kalyna, M. (2012). Transcriptome survey reveals increased complexity of the alternative splicing landscape in *Arabidopsis*. Genome Res. **22:** 1184–1195.

Michaels, S.D., and Amasino, R.M. (1999). FLOWERING LOCUS C encodes a novel MADS domain protein that acts as a repressor of flowering. Plant Cell **11:** 949–956.

Mockler, T.C., Yu, X., Shalitin, D., Parikh, D., Michael, T.P., Liou, J., Huang, J., Smith, Z., Alonso, J.M., Ecker, J.R., Chory, J., and Lin, C. (2004). Regulation of flowering time in *Arabidopsis* by K homology domain proteins. Proc. Natl. Acad. Sci. USA **101:** 12759–12764.

Nicholson, P., Yepiskoposyan, H., Metze, S., Zamudio Orozco, R., Kleinschmidt, N., and Mühlemann, O. (2010). Nonsense-mediated mRNA decay in human cells: mechanistic insights, functions beyond quality control and the double-life of NMD factors. Cell. Mol. Life Sci. **67:** 677–700.

Nilsen, T.W., and Graveley, B.R. (2010). Expansion of the eukaryotic proteome by alternative splicing. Nature **463:** 457–463.

Ossowski, S., Schwab, R., and Weigel, D. (2008). Gene silencing in plants using artificial microRNAs and other small RNAs. Plant J. **53:** 674–690.

Palusa, S.G., Ali, G.S., and Reddy, A.S. (2007). Alternative splicing of pre-mRNAs of *Arabidopsis* serine/arginine-rich proteins: regulation by hormones and stresses. Plant J. **49:** 1091–1107.

Palusa, S.G., and Reddy, A.S. (2010). Extensive coupling of alternative splicing of pre-mRNAs of serine/arginine (SR) genes with nonsense-mediated decay. New Phytol. **185:** 83–89.

Pan, Q., Shai, O., Lee, L.J., Frey, B.J., and Blencowe, B.J. (2008). Deep surveying of alternative splicing complexity in the human transcriptome by high-throughput sequencing. Nat. Genet. **40:** 1413–1415.

Penfield, S., Josse, E.M., and Halliday, K.J. (2010). A role for an alternative splice variant of PIF6 in the control of *Arabidopsis* primary seed dormancy. Plant Mol. Biol. **73:** 89–95.

Penfield, S., Josse, E.M., Kannangara, R., Gilday, A.D., Halliday, K.J., and Graham, I.A. (2005). Cold and light control seed germination through the bHLH transcription factor SPATULA. Curr. Biol. **15:** 1998–2006.

Raczynska, K.D., Simpson, C.G., Ciesiolka, A., Szewc, L., Lewandowska, D., McNicol, J., Szweykowska-Kulinska, Z., Brown, J.W., and Jarmolowski, A. (2010). Involvement of the nuclear cap-binding protein complex in alternative splicing in *Arabidopsis thaliana*. Nucleic Acids Res. **38:** 265–278.

Ratcliffe, O.J., Nadzan, G.C., Reuber, T.L., and Riechmann, J.L. (2001). Regulation of flowering in *Arabidopsis* by an FLC homologue. Plant Physiol. **126:** 122–132.

Reddy, A.S. (2007). Alternative splicing of pre-messenger RNAs in plants in the genomic era. Annu. Rev. Plant Biol. **58:** 267–294.

Reddy, A.S., Rogers, M.F., Richardson, D.N., Hamilton, M., and Ben-Hur, A. (2012). Deciphering the plant splicing code: experimental and computational approaches for predicting alternative splicing and splicing regulatory elements. Front. Plant Sci. **3:** 18.

Reddy, A.S., and Shad Ali, G. (2011). Plant serine/arginine-rich proteins: Roles in precursor messenger RNA splicing, plant development, and stress responses. Wiley Interdiscip. Rev. RNA **2:** 875–889.

Sanchez, S.E., et al. (2010). A methyl transferase links the circadian clock to the regulation of alternative splicing. Nature **468:** 112–116.

Saulière, J., Sureau, A., Expert-Bezançon, A., and Marie, J. (2006). The polypyrimidine tract binding protein (PTB) represses splicing of exon 6B from the beta-tropomyosin pre-mRNA by directly interfering with the binding of the U2AF65 subunit. Mol. Cell. Biol. **26:** 8755–8769.

Sawicka, K., Bushell, M., Spriggs, K.A., and Willis, A.E. (2008). Polypyrimidine-tract-binding protein: a multifunctional RNA-binding protein. Biochem. Soc. Trans. **36:** 641–647.

Schneider, C.A., Rasband, W.S., and Eliceiri, K.W. (2012). NIH Image to ImageJ: 25 years of image analysis. Nat. Methods **9:** 671–675.

Schöning, J.C., Streitner, C., Meyer, I.M., Gao, Y., and Staiger, D. (2008). Reciprocal regulation of glycine-rich RNA-binding proteins via an interlocked feedback loop coupling alternative splicing to

nonsense-mediated decay in *Arabidopsis*. Nucleic Acids Res. **36:** 6977–6987.

Severing, E.I., van Dijk, A.D., Morabito, G., Busscher-Lange, J., Immink, R.G., and van Ham, R.C. (2012). Predicting the impact of alternative splicing on plant MADS domain protein function. PLoS ONE **7:** e30524.

Severing, E.I., van Dijk, A.D., Stiekema, W.J., and van Ham, R.C. (2009). Comparative analysis indicates that alternative splicing in plants has a limited role in functional expansion of the proteome. BMC Genomics **10:** 154.

Sharma, S., Falick, A.M., and Black, D.L. (2005). Polypyrimidine tract binding protein blocks the 5′ splice site-dependent assembly of U2AF and the prespliceosomal E complex. Mol. Cell **19:** 485–496.

Sheldon, C.C., Burn, J.E., Perez, P.P., Metzger, J., Edwards, J.A., Peacock, W.J., and Dennis, E.S. (1999). The FLF MADS box gene: a repressor of flowering in *Arabidopsis* regulated by vernalization and methylation. Plant Cell **11:** 445–458.

Simpson, C.G., Fuller, J., Maronova, M., Kalyna, M., Davidson, D., McNicol, J., Barta, A., and Brown, J.W. (2008). Monitoring changes in alternative precursor messenger RNA splicing in multiple gene transcripts. Plant J. **53:** 1035–1048.

Spellman, R., Llorian, M., and Smith, C.W. (2007). Crossregulation and functional redundancy between the splicing regulator PTB and its paralogs nPTB and ROD1. Mol. Cell **27:** 420–434.

Spellman, R., and Smith, C.W. (2006). Novel modes of splicing repression by PTB. Trends Biochem. Sci. **31:** 73–76.

Staiger, D., and Green, R. (2011). RNA-based regulation in the plant circadian clock. Trends Plant Sci. **16:** 517–523.

Staiger, D., Zecca, L., Wieczorek Kirk, D.A., Apel, K., and Eckstein, L. (2003). The circadian clock regulated RNA-binding protein AtGRP7 autoregulates its expression by influencing alternative splicing of its own pre-mRNA. Plant J. **33:** 361–371.

Stauffer, E., Westermann, A., Wagner, G., and Wachter, A. (2010). Polypyrimidine tract-binding protein homologues from *Arabidopsis* underlie regulatory circuits based on alternative splicing and downstream control. Plant J. **64:** 243–255.

Stegle, O., Drewe, P., Bohnert, R., Borgwardt, K.M., and Rätsch, G. (May 11, 2010). Statistical tests for detecting differential RNA-transcript expression from read counts. Nat. Preced. 10.1038/npre.2010.4437.1.

Streitner, C., Danisman, S., Wehrle, F., Schöning, J.C., Alfano, J.R., and Staiger, D. (2008). The small glycine-rich RNA binding protein AtGRP7 promotes floral transition in *Arabidopsis thaliana*. Plant J. **56:** 239–250.

Sugliani, M., Brambilla, V., Clerkx, E.J., Koornneef, M., and Soppe, W.J. (2010). The conserved splicing factor SUA controls alternative splicing of the developmental regulator ABI3 in *Arabidopsis*. Plant Cell **22:** 1936–1946.

Swiezewski, S., Liu, F., Magusin, A., and Dean, C. (2009). Cold-induced silencing by long antisense transcripts of an *Arabidopsis* Polycomb target. Nature **462:** 799–802.

Syed, N.H., Kalyna, M., Marquez, Y., Barta, A., and Brown, J.W. (2012). Alternative splicing in plants - Coming of age. Trends Plant Sci. **17:** 616–623.

Terzi, L.C., and Simpson, G.G. (2008). Regulation of flowering time by RNA processing. Curr. Top. Microbiol. Immunol. **326:** 201–218.

Thimm, O., Bläsing, O., Gibon, Y., Nagel, A., Meyer, S., Krüger, P., Selbig, J., Müller, L.A., Rhee, S.Y., and Stitt, M. (2004). MAPMAN: A user-driven tool to display genomics data sets onto diagrams of metabolic pathways and other biological processes. Plant J. **37:** 914–939.

Wachter, A. (2010). Riboswitch-mediated control of gene expression in eukaryotes. RNA Biol. **7:** 67–76.

Wachter, A., Rühl, C., and Stauffer, E. (2012). The role of polypyrimidine tract-binding proteins and other hnRNP proteins in plant splicing regulation. Front. Plant Sci. **3:** 81.

Wachter, A., Tunc-Ozdemir, M., Grove, B.C., Green, P.J., Shintani, D.K., and Breaker, R.R. (2007). Riboswitch control of gene expression in plants by splicing and alternative 3′ end processing of mRNAs. Plant Cell **19:** 3437–3450.

Wang, B.B., and Brendel, V. (2006). Genomewide comparative analysis of alternative splicing in plants. Proc. Natl. Acad. Sci. USA **103:** 7175–7180.

Wang, S., and Okamoto, T. (2009). Involvement of polypyrimidine tract-binding protein (PTB)-related proteins in pollen germination in *Arabidopsis*. Plant Cell Physiol. **50:** 179–190.

Wollerton, M.C., Gooding, C., Wagner, E.J., Garcia-Blanco, M.A., and Smith, C.W. (2004). Autoregulation of polypyrimidine tract binding protein by alternative splicing leading to nonsense-mediated decay. Mol. Cell **13:** 91–100.

Xue, Y., Zhou, Y., Wu, T., Zhu, T., Ji, X., Kwon, Y.S., Zhang, C., Yeo, G., Black, D.L., Sun, H., Fu, X.D., and Zhang, Y. (2009). Genome-wide analysis of PTB-RNA interactions reveals a strategy used by the general splicing repressor to modulate exon inclusion or skipping. Mol. Cell **36:** 996–1006.

Yap, K., Lim, Z.Q., Khandelia, P., Friedman, B., and Makeyev, E.V. (2012). Coordinated regulation of neuronal mRNA steady-state levels through developmentally controlled intron retention. Genes Dev. **26:** 1209–1223.

Zenoni, S., Ferrarini, A., Giacomelli, E., Xumerle, L., Fasoli, M., Malerba, G., Bellin, D., Pezzotti, M., and Delledonne, M. (2010). Characterization of transcriptional complexity during berry development in *Vitis vinifera* using RNA-Seq. Plant Physiol. **152:** 1787–1795.

Zhang, G., et al. (2010). Deep RNA sequencing at single base-pair resolution reveals high complexity of the rice transcriptome. Genome Res. **20:** 646–654.